NIH Public Access
Author Manuscript
Nat Commun. Author manuscript; available in PMC 2013 December 25.

Published in final edited form as:
Nat Commun. 2013 June 25; 4: 2030. doi:10.1038/ncomms3030.

Scara1 deficiency impairs clearance of soluble Amyloid-β by mononuclear phagocytes and accelerates Alzheimer's-like disease progression

Dan Frenkel[1,¶,*], **Kim Wilkinson**[2,¶], **Lingzhi Zhao**[2], **Suzanne E. Hickman**[2], **Terry K. Means**[2], **Lindsey Puckett**[2], **Dorit Farfara**[1], **Nathan D. Kingery**[1], **Howard L. Weiner**[3], and **Joseph El Khoury**[2,4,*]

[1]Department of Neurobiology, George S. Wise Faculty of Life Sciences, Tel Aviv University, Tel Aviv, Israel

[2]Center for Immunology and Inflammatory Diseases, Massachusetts General Hospital, Harvard Medical School, CNY 149, Room 8301, 149 13th Street, Charlestown, Massachusetts 02129, USA

[3]Center for Neurologic Diseases, Brigham and Women's Hospital, Harvard Medical School, Boston, MA 02115, USA

[4]Division of Infectious Diseases, Massachusetts General Hospital, Harvard Medical School, CNY 149, Room 8301, 149 13th Street, Charlestown, Massachusetts 02129, USA

Abstract

In Alzheimer's disease soluble amyloid beta (sAβ) causes synaptic dysfunction and neuronal loss. Receptors involved in clearance of sAβ are not known. Here we use shRNA screening and identify the scavenger receptor *Scara1* as a receptor for sAβ expressed on myeloid cells. To determine the role of *Scara1* in clearance of sAβ *in vivo*, we cross *Scara1* null mice with PS1-APP mice, a mouse model of Alzheimer's disease and generate PS1-APP- *Scara1*-deficient mice. *Scara1* deficiency markedly accelerates Aβ accumulation leading to increased mortality. In contrast, pharmacological upregulation of *Scara1* expression on mononuclear phagocytes increases Aβ clearance. This approach is a potential treatment strategy for Alzheimer's disease.

Keywords

Microglia; monocytes; Alzheimer's disease; Transgenic mice; Amyloid; Phagocytosis; Degradation; Protollin; Scavenger receptor

Introduction

Work in transgenic mouse models of Alzheimer's disease (AD) indicates that mononuclear phagocytes can promote the clearance of amyloid-β (Aβ) peptides. Reduction in the number

*Correspondence should be addressed to JEK (jelkhoury@partners.org) or DF (dfrenkel@tauex.tau.ac.il).
¶Contributed equally to the work.

Author Contributions
DF and KW designed, performed and analyzed experiments. LZ, SH, TK, LP, DF, NK, performed and analyzed experiments, HLW designed experiments and edited manuscript, JEK designed, supervised and analyzed experiments, and wrote the manuscript.

Competing Financial Interests
The authors have no competing financial interests.

NIH-PA Author Manuscript
NIH-PA Author Manuscript
NIH-PA Author Manuscript

NIH-PA Author Manuscript

NIH-PA Author Manuscript

NIH-PA Author Manuscript

of recruited mononuclear phagocyte led to accelerated Aβ deposition especially around blood vessels, leading to intracerebral hemorrhage and increased mortality in a mouse model of AD[1]. In support of these findings, depletion of perivascular macrophages significantly increased the number of Thioflavin S-positive cortical blood vessels and total perivascular Aβ levels[2]. Conversely, stimulation of perivascular macrophage turnover or enhancing recruitment of peripheral monocytes reduced cerebral perivascular and parenchymal Aβ load[2, 3]. These data suggest that mononuclear phagocytes may delay progression of AD by promoting clearance of Aβ and preventing senile plaque formation. However, persistent Aβ accumulation in spite of increasing mononuclear phagocyte numbers in AD suggests that the ability of these cells to clear Aβ may decrease with age and progression of AD pathology[4].

Much attention has been focused for many years on the insoluble aggregates of Aβ found in senile plaques. Insoluble fibrillar aggregates are neurotoxic *in vitro* and activate microglia and astrocytes to produce cytokines, chemokines and reactive oxygen and nitrogen species[5], however, the number of senile plaques in any particular areas of the brain does not always correlate with neuronal death or synaptic loss in that area[6–8]. Such discrepancy brought attention to other non-aggregated forms of Aβ[9, 10]. These soluble forms of Aβ (sAβ) include Aβ monomers or oligomers that remain soluble in aqueous buffers after high speed ultracentrifugation[9, 10]. sAβ may start accumulating in the brain before formation of visible senile plaques. sAβ is associated with cognitive dysfunction in transgenic mice and several groups confirmed that a strong correlation exists between sAβ levels and synaptic loss and neuronal degeneration[6–12]. It is not known whether sAβ interacts with monocytes or microglia or the potential receptors involved in such interactions. However, since sAβ starts accumulating before formation of senile plaques and microglia are constantly surveying their environment for any potential injurious stimuli[13] we hypothesized that mononuclear phagocytes can recognize and bind sAβ.

Microglia and macrophages express several receptors that can promote binding and/or phagocytosis of fibrillar Aβ aggregates *in vitro*. These include the class A1 scavenger receptors (*Scara1*)[14], the class B2 scavenger receptors (*Scarb2*) or CD36[5, 15], RAGE[16] and others. Mononuclear phagocytes also express a number of Aβ degrading enzymes, such as insulysin, neprilysin and others[4, 17]. The exact role of each of these receptors in development or progression of AD is not known. We found that as transgenic AD mice age, expression of these Aβ phagocytic receptors and Aβ degrading enzymes decreased significantly in microglia, thereby promoting Aβ accumulation and contributing to neurodegeneration[4]. This led us to hypothesize that restoring the ability of mononuclear phagocytes to phagocytose or degrade Aβ may be a therapeutic modality to delay or stop the progression of AD. In support of this hypothesis, genetic downregulation of the TGFβ-Smad2/3 innate immune signaling pathway, led to increased infiltration of macrophages around blood vessels, and decreased Aβ levels and behavioral deficits in AD mice[3]. It is not known if pharmacological stimulation of mononuclear phagocyte Aβ clearance pathways will also lead to mitigation of AD-like pathology.

In this paper we use a shRNA screen to identify receptors for sAβ and show that *Scara1* is a phagocytic receptor that mediates clearance of sAβ *in vitro*, and that *Scara1* deficiency is associated with increased early mortality and Aβ deposition in the PS1-APP mouse model of AD. We also show that pharmacological upregulation of *Scara1* leads to increased Aβ clearance suggesting that this approach may be a strategy for treatment of AD.

NIH-PA Author Manuscript

NIH-PA Author Manuscript

NIH-PA Author Manuscript

Results

ShRNA screen identifies Scara1 as a receptor for sAβ uptake

To identify mononuclear phagocyte receptors involved in the uptake of sAβ we used a mouse shRNA library targeting innate immune receptors to screen for genes that mediate macrophage uptake of sAβ labeled with the fluorescent dye Hilyte-Fluor 488. We confirmed that our Hilyte-Fluor 488 Aβ is soluble using native electrophoresis and Thioflavin S staining (Supplementary Fig. S1a,b) as described[5–8]. The RNAi Consortium has previously published that its lentiviral library silences genes in a diverse set of cell types, contains 5 shRNA for nearly every gene in the murine genome, and is capable of significantly reducing target mRNA levels (Fig. 1a)[18]. Using a subset of the mouse lentiviral shRNA library targeting toll-like receptors, scavenger receptors and other pattern recognition receptors[19], we performed a screen to identify genes that mediate macrophage uptake of sAβ 1–42-Hilyte Fluor 488 using RAW 264.7 (RAW) macrophages. Silencing expression of all receptors tested was effectively performed to ~20% of normal expression (Fig. 1a and not shown). Interestingly, only silencing of the scavenger receptors CD36 and *Scara1*, led to a significant reduction in sAβ 1–42-Hilyte Fluor 488 uptake by RAW macrophages (Fig. 1b and data not shown). The results of our shRNA screen indicate that *Scara1* and CD36 can mediate uptake of sAβ by mononuclear phagocytes *in vitro*. Gene silencing of other scavenger receptors such as *Scarb1, Scarf, CD68*, and *CXCL16* also expressed by macrophages, had no effect on uptake of sAβ 1–42-Hilyte Fluor 488 by RAW cells (Fig. 1b), suggesting that *Scara1* and CD36 are the main receptors involved in this process.

To confirm that uptake of sAβ by microglia is indeed a receptor-mediated event, we incubated N9 microglia with increasing concentrations of sAβ and quantified uptake by flow cytometry. As seen in fig.2a, uptake of sAβ by microglia began to reach saturation at ~2μM. In addition, uptake of sAβ by N9 microglia was time dependent and reached saturation at ~ 4 hours (Fig. 2b). These data indicate that uptake of sAβ by microglia is likely to be receptor-mediated and is saturable in a dose and time-dependent manner. To further confirm that uptake of sAβ by microglia is mediated by scavenger receptors, we incubated N9 cells for two hours with 1μM sAβ 1–42-Hilyte Fluor 488 ± 200μM Fucoidan, a broad inhibitor of scavenger receptors, and measured uptake by flow cytometry. Fucoidan significantly inhibited the amount of sAβ taken by N9 microglia (Fig. 2c) and the number of cells that took sAβ (Fig. 2d).

Scara1 deficiency is associated with reduced sAβ uptake

Expression of *Scara1* in HEK293 cells is sufficient to promote the ability of these cells to take Aβ (Supplementary Fig. S2). To determine if *Scara1* is necessary for uptake of sAβ by primary monocytes and microglia as suggested by our shRNA screen in macrophages, we isolated circulating monocytes and microglia from adult mice with targeted deletion of various scavenger receptors and from WT mice and tested the ability of these freshly isolated monocytes and microglia to take up sAβ. Interestingly, only targeted deletion of *Scara1*, led to a significant reduction in the uptake of sAβ by fresh monocytes (Fig, 3a) and microglia (Fig. 3b) by 65% and 50% respectively. Targeted deletion of CD36 did not affect uptake of sAβ by monocytes and only reduced its binding to microglia by 25%, which was not statistically significant. These data indicate that *Scara1* is a major receptor for uptake of sAβ by monocytes and microglia and that *Scara1*-mediated uptake is not redundant. The lack of effect of targeted deletion of CD36 on sAβ uptake suggests that unlike *Scara1*, CD36 does not play a non-redundant role in clearance of sAβ. Since targeted deletion of CD36 leads to reduced Aβ-induced activation of mononuclear phagocytes to produce cytokines and reactive oxygen species, our data suggest that CD36 may be involved in the activation of mononuclear phagocytes by sAβ and not in the clearance of sAβ by these cells[5, 20, 21].

NIH-PA Author Manuscript

NIH-PA Author Manuscript

NIH-PA Author Manuscript

This is reminiscent of the role CD36 plays in the interaction between macrophages and oxidized low density lipoproteins[22].

Increased mortality in PS1-APP-Scara1$^{-/-}$ mice

To determine if *Scara1* mediates clearance of sAβ *in vivo*, and the effects of such clearance on accumulation of Aβ we generated PS1-APP-*Scara1*$^{-/-}$ mice and analyzed these mice for Aβ levels and AD-like pathology. To accomplish this we utilized a strategy that we have successfully used in the past to generate transgenic APP mice deficient in the chemokine receptor Ccr2[1]. Briefly, PS1-APP mice on a C57BL6 background were crossed to *Scara1*$^{-/-}$ mice (also on a C57BL6 background) to generate PS1-APP-*Scara1*$^{+/-}$ mice. We then crossed these mice to *Scara1*$^{-/-}$ mice to generate PS1-APP-*Scara1*$^{-/-}$ mice. PS1-APP-*Scara1*$^{+/-}$ and PS1-APP-*Scara1*$^{-/-}$ mice initially appeared healthy, without obvious behavioral abnormalities. However, after reaching 7 weeks of age, there was a marked increase in the mortality rate of both PS1-APP-*Scara1*$^{+/-}$ and PS1-APP-*Scara1*$^{-/-}$ mice as compared to control PS1-APP mice (Fig. 4a). By 160 d of age, 39% of PS1-APP-*Scara1*$^{-/+}$ and 53% of PS1-APP-*Scara1*$^{-/-}$ mice had died, compared to 16% of PS1-APP mice. The number of dying PS1-APP-*Scara1*$^{+/-}$ mice reached a plateau at age 108 d, in contrast PS1-APP-*Scara1*$^{-/-}$ mice continued to die until our data collection had stopped by age 160d. And while PS1-APP-*Scara1*$^{-/-}$ mice had higher mortality at 160 days than PS1-APP-*Scara1*$^{+/-}$ mice the overall difference between those two genotypes did not reach statistical significance (Fig. 4a). These data show that *Scara1* deficiency leads to increased mortality in mice expressing the PS1-APP transgenes. These data are similar to what we found with *Ccr2* deficiency (a defect that leads to reduced mononuclear phagocyte recruitment but does not affect their function[1]). These data indicate that blocking mononuclear phagocyte number or function has detrimental effect in AD mouse models.

As expected, *Scara1* mRNA levels in the brains of PS1-APP-*Scara1*$^{+/-}$ mice were ~45% of those in PS1-APP mice and were not detectable in PS1-APP-*Scara1*$^{-/-}$ mice as determined by quantitative real-time PCR (qPCR) (Fig. 4b). A similar trend was observed in WT, *Scara1*$^{+/-}$ and *Scara1*$^{-/-}$ mice (not shown). Interestingly, analysis of *Scara1* protein expression by Western blot showed that 55% reduction in *Scara1* gene dosage (as occurs in *Scara1*$^{+/-}$ mice) is associated with a much larger 76% reduction in *Scara1* protein level (Fig. 4 c and d). Since survival of PS1-APP mice appears to correlate with *Scara1* expression, it is possible that efficient clearance of Aβ requires a certain threshold of *Scara1* expression, the disproportionate reduction in *Scara1* protein levels in Scara1$^{+/-}$ mice-likely below such threshold-may explain the comparable mortality rates between PS1-APP-*Scara1*$^{+/-}$ and PS1-APP-*Scara1*$^{-/-}$ mice.

Increased Aβ accumulation in PS1-APP-Scara1$^{-/-}$ mice

To determine the effect(s) of *Scara1* deficiency on AD like pathology, we analyzed the brains of 8 months old PS1-APP-*Scara1*$^{-/-}$ mice for Aβ deposition in comparison to PS1-APP mice. As seen in Fig.4e–g, *Scara1* deficiency led to a significant increase in the surface area fraction of the brain stained for Aβ in PS1-APP mice. As expected WT mice did not have any Aβ in their brain at this age (Fig. 2e). These data support the results obtained from our shRNA screen and from the experiments showing decreased uptake of sAβ *in vitro* by monocytes and microglia isolated from *Scara1*$^{-/-}$ mice (Fig.3a–b). The data further indicate that *Scara1* is a major receptor involved in endogenous clearance of Aβ and that deficiency in *Scara1*, as occurs in aging AD mice[4], is associated with increased Aβ levels.

Our shRNA screening data showed that CD36 can mediate uptake of sAβ. RAGE has been also shown to be a receptor for Aβ[16]. To determine if *Scara1* deficiency indirectly affected CD36 or RAGE expression, we measured CD36 and RAGE mRNA in young (150 days)

NIH-PA Author Manuscript

NIH-PA Author Manuscript

NIH-PA Author Manuscript

WT, *Scara1*$^{-/-}$, PS1-APP and PS1-APP-*Scara1*$^{-/-}$ brains by qPCR. As seen in Figure 5a, *Scara1* deficiency did not affect CD36 mRNA levels in *Scara1*$^{-/-}$ or PS1-APP-*Scara1*$^{-/-}$ brains. Furthermore, we did not detect any difference in expression of RAGE, in PS1-APP-*Scara1*$^{-/-}$ mice compared to PS1-APP mice (Not shown). These data indicate that increased Aβ deposition in PS1-APP-*Scara1*$^{-/-}$ brains are likely due to decreased *Scara1*-mediated Aβ clearance in these mice and not due to a change in expression of other Aβ receptors such as Cd36 and RAGE.

Aβ levels are also regulated by several Aβ-degrading enzymes such as neprilysin and insulysin[17]. To determine if increased Aβ levels in the brains of PS1-APP-*Scara1*$^{-/-}$ mice are associated with reduced expression of neprilysin and/or insulysin, we measured mRNA levels of these two enzymes in the brains of young (150 days) WT, *Scara1*$^{-/-}$, PS1-APP and PS1-APP-*Scara1*$^{-/-}$ mice. We found that expression of insulysin and neprilysin was comparable in WT and *Scara1*$^{-/-}$ mice. Interestingly, expression of neprilysin was significantly higher in young PS1-APP mice compared to WT mice suggesting that early in the disease process, uptake of Aβ may be associated with increased Aβ degradation. Expression of insulysin was also slightly higher in PS1-APP mice compared to WT mice, but the difference was small and did not reach statistical significance (Fig. 5b, c). In contrast, both neprilysin and insulin expression was significantly reduced by 38% and 36% respectively in PS1-APP-*Scara1*$^{-/-}$ brains as compared to PS1-APP brains (Fig. 5b,c). These data suggest that phagocytosis of Aβ in young PS1-APP mice is associated with increased Aβ degradation, whereas decreased uptake of Aβ, as occurs in PS1-APP-*Scara1*$^{-/-}$ mice, leads to decreased Aβ degradation and further increase in Aβ accumulation thereby initiating a self-propagating loop of events that lead to accelerated disease progression.

Data shown in figure 4a indicate that mortality of PS1-APP-*Scara1*$^{+/-}$ mice was only slightly better than that of PS1-APP-*Scara1*$^{-/-}$ but the difference did not reach statistical significance. To determine if partial *Scara1* deficiency also affected AD-like pathology, we analyzed the brains of young (150 days) PS1-APP-*Scara1*$^{+/-}$ mice for Aβ deposition in comparison to PS1-APP mice. As seen in supplementary figure S3a, PS1-APP-*Scara1*$^{+/-}$ mice exhibited a significant increase in Aβ levels as measured by ELISA (700 pg/mg brain protein vs. 1500 pg/mg protein $p<0.002$). This increase also correlated with increased visible Aβ deposits (Supplementary Fig. S3b and c).

Of note, the number of visible Aβ deposits in ~150 days old PS1-APP and PS1-APP-*Scara1*$^{+/-}$ mice were small (Supplementary Fig. S3b and c), and we did not detect any Thioflavin S+ deposits (not shown) suggesting that the majority of Aβ measured in these mice is in soluble or non-aggregated form. These data support the results obtained from our shRNA screen and from the experiments showing decreased uptake of sAβ *in vitro* by monocytes and microglia isolated from *Scara1* deficient mice.

Upregulation of Scara1 leads to increased Aβ clearance

Protollin, a proteosome-based adjuvant comprised of purified outer membrane proteins of *Neisseria meningitides* and lipopolysaccharide that is well tolerated in humans[23], promotes increased accumulation of mononuclear phagocytes and increased clearance of amyloid when given intranasally to transgenic AD mice[24, 25]. We investigated whether the mechanism by which Protollin enhances Aβ uptake by mononuclear phagocytes involves upregulation of *Scara1* or CD36. As seen in figure 6a–c, while Protollin upregulated mRNA levels of *Scara1* by more than 3 fold, it didn't affect mRNA levels of CD36. Furthermore, Protollin upregulated *Ccl2* mRNA levels by ~7fold (Fig. 6d). These data suggest that the increased numbers of mononuclear phagocytes observed in Protollin treated Alzheimer's mice, may be due to their recruitment to sites of Aβ deposition via Ccl2. These data also

NIH-PA Author Manuscript

NIH-PA Author Manuscript

NIH-PA Author Manuscript

suggest that Protollin-induced enhanced Aβ clearance, may in part be due to increased recruitment of mononuclear phagocytes to Aβ deposition sites.

Clearance of Aβ deposits *in situ* from brain sections derived from transgenic AD mice has been used as a surrogate measure for astrocyte ability to clear Aβ *in vivo*[26]. To test if Protollin-induced activation of N9 microglia, promotes the ability of these cells to reduce Aβ deposits, we incubated these cells with brain sections derived from aged transgenic PS1-APP brains in the presence of increasing concentrations of Protollin. Such sections normally exhibit florid Aβ deposits in the cortex and hippocampus. As seen in figures 6e and 6f, the addition of Protollin-stimulated N9 microglia, significantly reduced the size and number of Aβ deposits in such sections in the hippocampus when compared to untreated sections, or to sections incubated with unstimulated N9 microglia. To determine the relative importance of *Scara1* in Aβ clearance by microglia activated with Protollin, we isolated WT and *Scara1*$^{-/-}$ adult microglia as previously described[26] and compared their ability to clear brain Aβ deposits from PS1-APP brain slices as we did with N9 cells. After incubation of the brain sections with microglia from WT mice for 72 h, there was a 58% reduction in total Aβ deposits in the hippocampus (p=0.0013) as compared to untreated sections and to sections incubated with microglia from *Scara1*$^{-/-}$ mice (p=0.0214), which showed only a 20% reduction (p=0.0317) as compared to untreated section (Fig. 6g,h). These data strongly support that Protollin-induced increased Aβ clearance is in part dependent on *Scara1* and that pharmacologic upregulation of *Scara1* expression can be successfully accomplished.

Discussion

The role of mononuclear phagocytes including peripheral monocytes and microglia in Alzheimer's disease is subject to intense investigation[27]. While a shotgun approach that deletes all microglia for a brief period of time did not show an effect on amyloid deposition in a transgenic AD mouse model[28], targeted genetic manipulation of the innate immune system in mouse models of Alzheimer's disease provided strong evidence that mononuclear phagocytes play critical roles in regulating Aβ deposition by regulating Aβ clearance pathways. Indeed, defects in microglial/mononuclear phagocytes accumulation in transgenic APP mice and other mouse models of AD are associated with increased Aβ deposition and increased mortality and/or cellular toxicity in these mice[1, 29]. Furthermore, deficiencies and/or mutations in specific innate immune receptors such as CD14 and TLR4 affect Aβ deposition[30, 31]. Unfortunately, with aging and progression of Alzheimer's disease, innate immune cells of the brain appear to become dysfunctional and their ability to clear amyloid becomes significantly reduced[4]. The exact mechanism(s) of such microglial dysfunction are not clear, but are believed to be due at least in part to downregulation of microglial Aβ phagocytic receptors[4]. In this manuscript, we provide direct evidence that the microglial/monocyte scavenger receptor *Scara1* is a key Aβ clearance receptor expressed by these cells and that genetic deficiency in *Scara1* is indeed associated with increased accumulation of Aβ. In addition, deficiency in *Scara1* is associated with increased mortality in PS1-APP mice. Such increases in mortality and Aβ deposition are similar to what we observed with APP-Ccr2-deficient mice and suggest that abnormalities in the number and/or function of mononuclear phagocytes can have detrimental effects on transgenic mouse models of AD. In contrast to the detrimental effects associated with dysfunction of the innate immune system in AD, we also show that restoring some of the Aβ-clearing ability of the innate immune system by pharmacological upregulation of *Scara1* leads to increased Aβ clearance by mononuclear phagocytes and microglia and therefore may be beneficial in slowing down or delaying progression of this disease. It is not clear if upregulating *Scara1* expression by non-pharmacological approaches will also lead to increased sAβ clearance. Indeed, upregulating *Scara1* mRNA in aging AD mice following irradiation does not seem to have the same effect as using Protollin[32]. It is possible that such apparent discrepancy may be due to increased

NIH-PA Author Manuscript

NIH-PA Author Manuscript

NIH-PA Author Manuscript

influx of Aβ across the blood brain barrier (BBB) as a result of increased permeability of the BBB following irradiation, to differences in the age and genotype of the mice analyzed and/or the approach used to quantify sAβ. Nonetheless, our data clearly indicate that upregulating *Scara1* expression pharmacologically, is a viable therapeutic strategy to treat AD.

We showed previously that blocking CD36-Aβ interactions reduces Aβ-induced activation of microglia to produce cytokines and reactive oxygen species[5, 20]. We also showed that blocking these interactions does not affect phagocytosis of Aβ. Therefore data from these papers indirectly support our findings in this manuscript that *Scara1* rather than CD36 is the main receptor for clearance of Aβ by mononuclear phagocytes. Our data also suggest that *Scara1* and CD36 play complementary non-redundant roles in the interactions of mononuclear phagocytes with Aβ. *Scara1*-Aβ interactions are beneficial and promote phagocytosis and clearance of Aβ, whereas, CD36-Aβ interactions are harmful and lead to production of neurotoxins and pro-inflammatory molecules. This is reminiscent of the role CD36 plays in the interaction between macrophages and oxidized low density lipoproteins in atherosclerosis. Indeed we have shown in the past that while *Scara1* mediates adhesion to Oxidized LDL coated surfaces, CD36 mediates macrophage activation by Oxidized LDL to produce reactive oxygen species[22]. In this regard the findings presented in this manuscript draw an exciting not yet described parallel between atherosclerosis and AD. Dissecting the complex roles of various scavenger receptors in mononuclear phagocyte-Aβ interactions is therefore very important and as we are showing in this manuscript has therapeutic implications for AD.

Materials and Methods

shRNA lentiviral infections

Plasmids encoding lentiviruses expressing shRNAs were obtained from the RNAi Consortium (TRC) library TRC-Mm1.0[18], purified using the QiaPrep miniprep kit (Qiagen) then transfected into HEK 293T cells with a three-plasmid system to produce lentivirus. Infection conditions were optimized in 96-well plates. 20,000 macrophages were placed in each well of 96-well tissue culture dishes and infected using 5 μl of shRNA lentiviral supernatant and 7.5 μg/ml polybrene. The cells were spun for 30 minutes at 2000 rpm and incubated for 24 hours. To select for shRNA integration, infected cells were placed in puromycin (3 μg/ml) and RPMI containing 10% FBS. The cells were tested 1–2 weeks after infection.

Mice—PS1-APP mice bi-transgenic mice (B6C3-Tg (APPswe, PSEN1dE9)85Dbo/J stock number 004462)[33, 34] were purchased from The Jackson Laboratories (Bar Harbor, ME) and bred in the animal care facilities at Massachusetts General Hospital. Control mice are non-transgenic littermates of those PS1-APP mice expressing these transgenes.

Scara1$^{-/-}$ mice were generated by professor Tatsuhiko Kodama, and a colony has been maintained in our lab for many years[35]. CD36$^{-/-}$ mice were generated by Dr. Kathryn Moore on a C57BL6 background and a colony has been maintained in our lab for many years[5]. PS1-APP, *Scara1*$^{-/-}$ and CD36$^{-/-}$ mice were backcrossed >13 generations on a C57BL/6 background.*Lox-1*$^{-/-}$ mice[36] were a generous gift from professor Tatsuya Sawamura, National Cardiovascular Center Research Institute Osaka, JAPAN. *RAGE*$^{-/-}$ mice[37] were a generous gift from professor Hiroshi Yamamoto, Kanazawa, Japan.

All protocols were approved by the Massachusetts General Hospital and Brigham and Women's Hospital Institutional Animal Care and Use Committees and met US National Institutes of Health guidelines for the humane care of animals.

NIH-PA Author Manuscript

NIH-PA Author Manuscript

NIH-PA Author Manuscript

Stimulation and cell surface staining of N9 microglia

N9 mouse microglia (a gift from Dr. P. Riciarrdi-Castagnoli, University of Milano, Bicocca, Italy)[38] were plated on 24-well plates coated with 1μg Fibronectin/cm^2 (Sigma-Aldrich), and grown overnight in RPMI supplemented with10% FBS, L-glutamine (2mM), penicillin 10 IU/ml and streptomycin 10μg/ml. The following day, Protollin (Glaxo Smith Kline, Laval, Quebec, Canada) was added and cells were incubated overnight. For staining, cells were lifted from the plate with CellStripper™ (Mediatech), and resuspended in PBS/1% BSA/2% FBS containing 10ug/ml Fc block (AbD Serotec) then APC-labeled anti-mouse CD11b (1μg/ml) (BD Biosciences Pharmingen, San Diego, CA) or APC-labeled hamster anti-mouse CD36 clone HM36 (1μg/ml) (BioLegend, San Diego, CA) or Alexa647-labeled anti-CD204 (Scara1) clone 2F8 (2.5 μg/ml) (AbD Serotec) or isotype-matched control antibodies (same concentrations as primary antibodies), were added and incubated on ice for 1 hour. Cells were then fixed and fluorescence intensity was measured using a FACScalibur™ (BD Biosciences, San Jose, CA) flow cytometer.

Isolation of $CD11b^+$ microglia from adult brains

Adult mouse microglia were isolated as described[4]. Briefly, 12 week old mice were euthanized and perfused with 30cc PBS without Ca^{++} and Mg^{++} ($PBS^{=}$). Brains were then rinsed, minced, and treated with Dispase and Collagenase Type 3 (Worthington Biochemicals, Lakewood, NJ), for 45 minutes at 37°C; followed by addition of 40U/ml DNase I grade II (Roche Applied Science, Indianapolis, IN) and incubation for an additional 15 minutes. The enzymes were inactivated by addition of 20ml Hanks Balanced Salt Solution without Ca^{++} and Mg^{++} ($HBSS^{=}$) (Mediatech) containing 2mM EDTA and 2% fetal bovine serum (FBS) and the digested brain bits were triturated sequentially with a 25-, 10-, and 5-ml pipette (8–10 times each step) and passed over a 100μm filter (Fisher Scientific, Pittsburgh, PA). Cells were centrifuged and resuspended in RPMI /L glutamine and mixed with physiologic Percoll® (Sigma Aldrich), and centrifuged at 850×g for 45 minutes. The cell pellet was resuspended in RPMI and the cells were passed over a 70μm filter (Fisher Scientific), washed then passed over a 40μm filter (Fisher Scientific). The cells were then incubated with anti-mouse Cd11b-coated microbeads (Miltenyi Biotech, Auburn, CA) then washed. The bead-cell pellet was resuspended in PBS/0.5% BSA/2mM EDTA and passed over a magnetic MACS® Cell Separation column (Miltenyi Biotech) to separate Cd11b-positive cells (i.e. cells that bound the beads–microglia/mononuclear phagocytes) from unbound Cd11b-negative cells ($CD11b^{neg}$. Flow-through was collected and the column was rinsed 3× with PBS/BSA/EDTA. CD11b-positive cells ($CD11b^+$) were eluted by removing the column from the magnetic holder and pushing PBS/BSA/EDTA through the column with a plunger. Cells were centrifuged and the pellets were resuspended in RPMI 1640 (Invitrogen) and used for experiments. Microglia isolated in this manner are more than 96% pure[4].

Isolation of Monocytes from WT and KO mice

Monocytes were isolated by centrifugation over Ficoll 1077 as described for human monocytes[39, 40]. This step removes neutrophils and red blood cells. The remaining cells include monocytes and Lymphocytes. This was followed by adhesion to tissue culture plates for 1 hour. The adherent cells (>90% monocytes) were then detached by brief incubation with 5 mM EDTA in PBS as described[39].

Quantitative Real Time PCR

Total RNA from each sample of cells (7.5–15 $\times 10^5$ cells) was isolated using the RNeasy® Plus mini kit (Qiagen, Valencia, CA) according to the manufacturer's instructions and reverse transcribed using Multiscribe™ reverse transcriptase (Applied Biosystems, Foster

NIH-PA Author Manuscript

NIH-PA Author Manuscript

NIH-PA Author Manuscript

City, CA). Dilutions of each cDNA prep were used to assess β2-microglobulin RNA levels and samples were then adjusted to give equivalent levels of β2-microglobulin per well in subsequent qPCR reactions for other genes. The qPCR was performed with the MX4000™ unit (Agilent technologies, Santa Clara, CA) using SYBR Green to detect the amplification products as described[1, 5]. The following cycles were performed: initial denaturation cycle 95°C for 10 min, followed by 40 amplification cycles of 95°C for 15 secs and 60°C for one min and ending with one cycle at 25°C for 15 secs. Relative quantification of mRNA expression was calculated by the comparative cycle method described by the manufacturer (Agilent technologies).

For *Scara1* qPCR, a standard curve for *Scara1* was prepared from a plasmid (Open Biosystems, Huntsville, AL) containing full-length mouse *Scara1* then whole brain RNA was isolated from triplicate samples using a Qiagen RNA easy Mini kit (Valencia, CA) and quantified using a Thermo-Fisher Nanodrop (Waltham, MA). 1μg RNA was reverse-transcribed into cDNA using Invitrogen's First Strand Synthesis kit (Carlsbad, CA), and qPCR performed in a Roche 480 Lightcycler qPCR machine (Indianapolis, IN) in triplicates for *Scara1* (Forward primer: TGAACGAGAGGATGCTGACTG, Reverse primer: GGAGGGGCCATTTTTAGTGC) and compared to a standard curve of mouse *Scara1* cDNA

Aβ ELISA

For measurement of Aβ, we used commercially available ELISA kits (Invitrogen). Hemispheres of WT, PS1-APP and PS1-APP-*Scara1*$^{+/-}$ mice were homogenized in buffer containing 0.02 M guanidine and ELISA for Aβ performed according to the manufacturer's instructions.

In vitro uptake of Aβ by N9 cells

N9 cells cultured in 6 well plates were incubated overnight with various concentrations of Protollin. The cells were then incubated with PBS containing 1% BSA and 500ng/ml Aβ 1–42 labeled with Alexa 488 (Anaspec, CA) for up to 4 hours, then washed 3× in PBS and lifted from the plate with CellStripper™ (Mediatech). Cells were then fixed by the addition of 2% PFA. Cell associated fluorescence intensity was measured using a FACScalibur™ (BD Biosciences, San Jose, CA) flow cytometer.

Uptake of Aβ from brain sections and Immunohistochemistry

Brains from transgenic PS1-APP were harvested and frozen unfixed in liquid nitrogen vapor and stored at −80°C and 10–14μm frozen sections were cut. N9 cells or WT microglia isolated from adult mice, were then added in the presence of Protollin and incubated at 37°C for 24 hours. Unbound cells were then rinsed in PBS and the sections fixed in 4% PFA. To stain for Aβ, sections were blocked in PBS / 0.3%Triton-X 100 / 2% goat serum for 30 minutes, then incubated overnight at 25°C with rabbit anti-pan Aβ antibody (Biosource, Camarillo, CA) or control antibody, at 2μg/ml in PBS containing 0.3% Triton X-100 and 2% goat serum. The slides were then processed using the Vectastain® Elite ABC Kit Rabbit IgG (Vector laboratories, Burlingame, CA) according to the manufacturer's instructions. Vector ® NovaRed™ substrate kit for peroxidase (Vector Laboratories) was used to develop target-bound peroxidase for detection of Aβ in brain sections. Slides were counterstained with hematoxylin, mounted with VectaMount® (Vector Laboratories), visualized by brightfield microscopy and digitally photographed. Alternatively, secondary anti rabbit IgG antibodies labeled with Alexa488™ were used, the slides counterstained with DAPI and mounted using Vectashield® (Vector Laboratories) and digitally photographed. For quantitation of the percent surface area stained with Anti-Aβ, 5 equally spaced sections were used per brain.

NIH-PA Author Manuscript

NIH-PA Author Manuscript

NIH-PA Author Manuscript

Western blot of Scara1

2μg cell lysates were loaded onto a 10% SDS polyacrylamide gel (Invitrogen) transferred via iBlot® (Invitrogen) onto polyvinylidene difluoride (PVDF) membrane, blocked for 1 hour with 5% milk, then incubated with primary goat anti- mouse *Scara1* antibodies (R&D systems) followed by anti-goat horseradish peroxidase –labeled secondary antibody. The blots were then exposed to Hyperfilm™ (Amersham), developed and band intensity quantified by densitometry with image J software.

Statistical analysis

Statistical analysis was performed using one-way ANOVA with the Tukey test provided in the “Microcal Origin 8” graphics and statistics software. P values<0.05 where considered significant.

Supplementary Material

Refer to Web version on PubMed Central for supplementary material.

Acknowledgments

This work was supported by a grant from the HFSP and ISF and an NIRG grant from the Alzheimer’s Association to DF, by grant AG043975 to HLW and by NIH grants NS059005, AG032349, AI082660 and a grant from the Dana Foundation Neuroimmunology Program to JEK.

References

1. El Khoury J, et al. Ccr2 deficiency impairs microglial accumulation and accelerates progression of Alzheimer-like disease. Nat Med. 2007; 13:432–438. [PubMed: 17351623]
2. Hawkes CA, McLaurin J. Selective targeting of perivascular macrophages for clearance of beta-amyloid in cerebral amyloid angiopathy. Proc Natl Acad Sci U S A. 2009; 106:1261–1266. [PubMed: 19164591]
3. Town T, et al. Blocking TGF-beta-Smad2/3 innate immune signaling mitigates Alzheimer-like pathology. Nat Med. 2008; 14:681–687. [PubMed: 18516051]
4. Hickman SE, Allison EK, El Khoury J. Microglial dysfunction and defective beta-amyloid clearance pathways in aging Alzheimer's disease mice. J Neurosci. 2008; 28:8354–8360. [PubMed: 18701698]
5. El Khoury JB, et al. CD36 mediates the innate host response to beta-amyloid. J Exp Med. 2003; 197:1657–1666. [PubMed: 12796468]
6. Lue LF, et al. Soluble amyloid beta peptide concentration as a predictor of synaptic change in Alzheimer's disease. Am J Pathol. 1999; 155:853–862. [PubMed: 10487842]
7. McLean CA, et al. Soluble pool of Abeta amyloid as a determinant of severity of neurodegeneration in Alzheimer's disease. Ann Neurol. 1999; 46:860–866. [PubMed: 10589538]
8. Wang J, Dickson DW, Trojanowski JQ, Lee VM. The levels of soluble versus insoluble brain Abeta distinguish Alzheimer's disease from normal and pathologic aging. Exp Neurol. 1999; 158:328–337. [PubMed: 10415140]
9. Haass C, Selkoe DJ. Soluble protein oligomers in neurodegeneration: lessons from the Alzheimer's amyloid beta-peptide. Nat Rev Mol Cell Biol. 2007; 8:101–112. [PubMed: 17245412]
10. Sakono M, Zako T. Amyloid oligomers: formation and toxicity of Abeta oligomers. Febs J. 277:1348–1358. [PubMed: 20148964]
11. Lesne S, et al. A specific amyloid-beta protein assembly in the brain impairs memory. Nature. 2006; 440:352–357. [PubMed: 16541076]
12. Walsh DM, et al. Naturally secreted oligomers of amyloid beta protein potently inhibit hippocampal long-term potentiation in vivo. Nature. 2002; 416:535–539. [PubMed: 11932745]

NIH-PA Author Manuscript

NIH-PA Author Manuscript

NIH-PA Author Manuscript

13. Nimmerjahn A, Kirchhoff F, Helmchen F. Resting microglial cells are highly dynamic surveillants of brain parenchyma in vivo. Science. 2005; 308:1314–1318. [PubMed: 15831717]
14. El Khoury J, et al. Scavenger receptor-mediated adhesion of microglia to beta-amyloid fibrils. Nature. 1996; 382:716–719. [PubMed: 8751442]
15. Coraci IS, et al. CD36, a class B scavenger receptor, is expressed on microglia in Alzheimer's disease brains and can mediate production of reactive oxygen species in response to beta-amyloid fibrils. Am J Pathol. 2002; 160:101–112. [PubMed: 11786404]
16. Yan SD, et al. RAGE and amyloid-beta peptide neurotoxicity in Alzheimer's disease. Nature. 1996; 382:685–691. [PubMed: 8751438]
17. El Khoury Joseph, HSE. Mechanisms of Amyloid B clearance in Alzheimer's disease. Sun, M-K., editor. New York: Nova Biomedical Books; 2009.
18. Moffat J, et al. A lentiviral RNAi library for human and mouse genes applied to an arrayed viral high-content screen. Cell. 2006; 124:1283–1298. [PubMed: 16564017]
19. Means TK, et al. Evolutionarily conserved recognition and innate immunity to fungal pathogens by the scavenger receptors SCARF1 and CD36. J Exp Med. 2009; 206:637–653. [PubMed: 19237602]
20. Wilkinson K, Boyd JD, Glicksman M, Moore KJ, El Khoury J. A high-content drug screen identifies ursolic acid as an inhibitor of amyloid-{beta} interactions with its receptor CD36. J Biol Chem.
21. Stewart CR, et al. CD36 ligands promote sterile inflammation through assembly of a Toll-like receptor 4 and 6 heterodimer. Nat Immunol. 11:155–161. [PubMed: 20037584]
22. Maxeiner H, et al. Complementary roles for scavenger receptor A and CD36 of human monocyte-derived macrophages in adhesion to surfaces coated with oxidized low-density lipoproteins and in secretion of H2O2. J Exp Med. 1998; 188:2257–2265. [PubMed: 9858512]
23. Fries LF, et al. Safety and immunogenicity of a proteosome-Shigella flexneri 2a lipopolysaccharide vaccine administered intranasally to healthy adults. Infect Immun. 2001; 69:4545–4553. [PubMed: 11401998]
24. Frenkel D, Maron R, Burt DS, Weiner HL. Nasal vaccination with a proteosome-based adjuvant and glatiramer acetate clears beta-amyloid in a mouse model of Alzheimer disease. J Clin Invest. 2005; 115:2423–2433. [PubMed: 16100572]
25. Frenkel D, et al. A nasal proteosome adjuvant activates microglia and prevents amyloid deposition. Ann Neurol. 2008; 63:591–601. [PubMed: 18360829]
26. Wyss-Coray T, et al. Adult mouse astrocytes degrade amyloid-beta in vitro and in situ. Nat Med. 2003; 9:453–457. [PubMed: 12612547]
27. El Khoury J. Neurodegeneration and the neuroimmune system. Nat Med. 16:1369–1370. [PubMed: 21135838]
28. Grathwohl SA, et al. Formation and maintenance of Alzheimer's disease beta-amyloid plaques in the absence of microglia. Nat Neurosci. 2009; 12:1361–1363. [PubMed: 19838177]
29. Bruban J, et al. CCR2/CCL2-mediated inflammation protects photoreceptor cells from amyloid-beta-induced apoptosis. Neurobiol Dis. 42:55–72. [PubMed: 21220018]
30. Reed-Geaghan EG, Reed QW, Cramer PE, Landreth GE. Deletion of CD14 attenuates Alzheimer's disease pathology by influencing the brain's inflammatory milieu. J Neurosci. 30:15369–15373. [PubMed: 21084593]
31. Song M, et al. TLR4 mutation reduces microglial activation, increases Abeta deposits and exacerbates cognitive deficits in a mouse model of Alzheimer's disease. J Neuroinflammation. 8:92. [PubMed: 21827663]
32. Mildner A, et al. Distinct and non-redundant roles of microglia and myeloid subsets in mouse models of Alzheimer's disease. J Neurosci. 31:11159–11171. [PubMed: 21813677]
33. Borchelt DR, et al. Accelerated amyloid deposition in the brains of transgenic mice coexpressing mutant presenilin 1 and amyloid precursor proteins. Neuron. 1997; 19:939–945. [PubMed: 9354339]
34. Jankowsky JL, et al. Co-expression of multiple transgenes in mouse CNS: a comparison of strategies. Biomol Eng. 2001; 17:157–165. [PubMed: 11337275]

NIH-PA Author Manuscript

NIH-PA Author Manuscript

NIH-PA Author Manuscript

35. Thomas CA, et al. Protection from lethal gram-positive infection by macrophage scavenger receptor-dependent phagocytosis. J Exp Med. 2000; 191:147–156. [PubMed: 10620613]

36. Mehta JL, et al. Deletion of LOX-1 reduces atherogenesis in LDLR knockout mice fed high cholesterol diet. Circ Res. 2007; 100:1634–1642. [PubMed: 17478727]

37. Yonekura H, Yamamoto Y, Sakurai S, Watanabe T, Yamamoto H. Roles of the receptor for advanced glycation endproducts in diabetes-induced vascular injury. J Pharmacol Sci. 2005; 97:305–311. [PubMed: 15750291]

38. El Khoury J, et al. Scavenger receptor-mediated adhesion of microglia to beta-amyloid fibrils. Nature. 1996; 382:716–719. [PubMed: 8751442]

39. el Khoury J, et al. Macrophages adhere to glucose-modified basement membrane collagen IV via their scavenger receptors. J Biol Chem. 1994; 269:10197–10200. [PubMed: 8144597]

40. Hickman SE, el Khoury J, Greenberg S, Schieren I, Silverstein SC. P2Z adenosine triphosphate receptor activity in cultured human monocyte-derived macrophages. Blood. 1994; 84:2452–2456. [PubMed: 7919365]

NIH-PA Author Manuscript

NIH-PA Author Manuscript

NIH-PA Author Manuscript

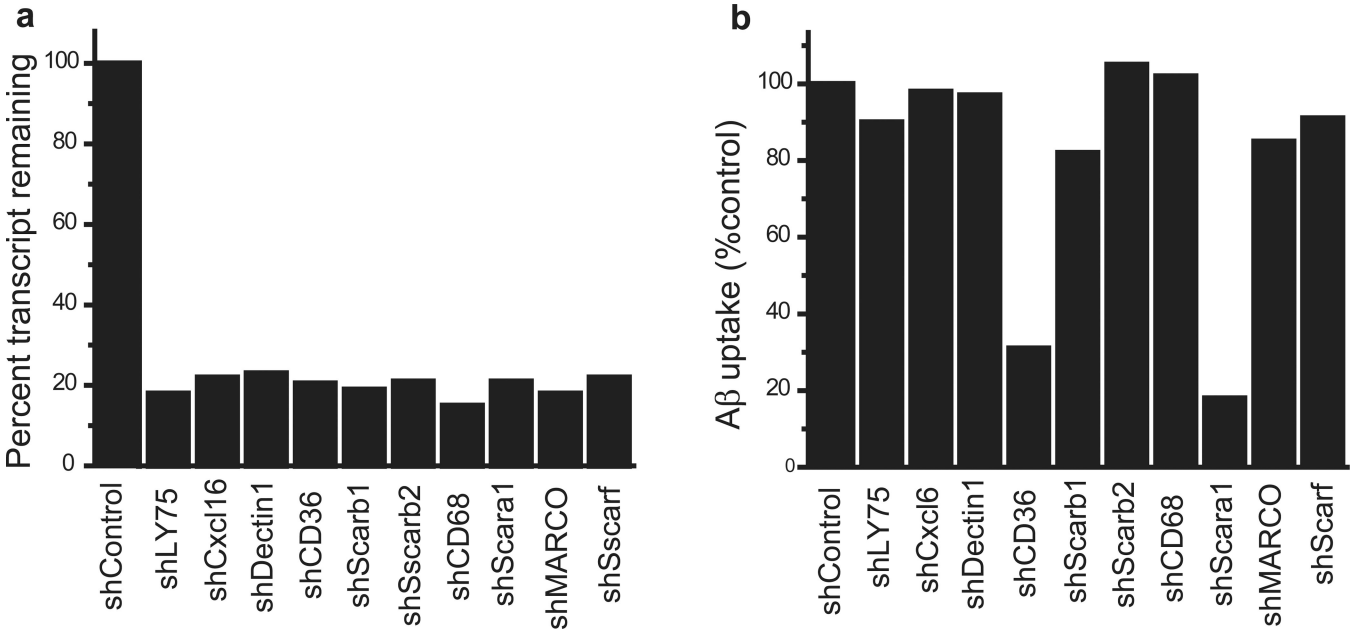

Figure 1. A shRNA screen identifies *Scara1* as a receptor for sAβ

(a) RAW macrophages were transduced with lentivirus encoding gene-specific shRNAs to 30 pattern recognition receptors or with a control shRNA directed against GFP. Gene expression was measured by qPCR, and three to five individual shRNAs per gene were identified that significantly reduced mRNA expression. **(b)** Pattern recognition receptor expression was knocked down in individual pools of RAW macrophages, which were then incubated with Hilyte-fluor labeled sAβ1–42 for 2 h. Cell associated sAβ was then quantified by flow cytometry. Data are from a representative experiments repeated 3 times with similar results.

NIH-PA Author Manuscript

NIH-PA Author Manuscript

NIH-PA Author Manuscript

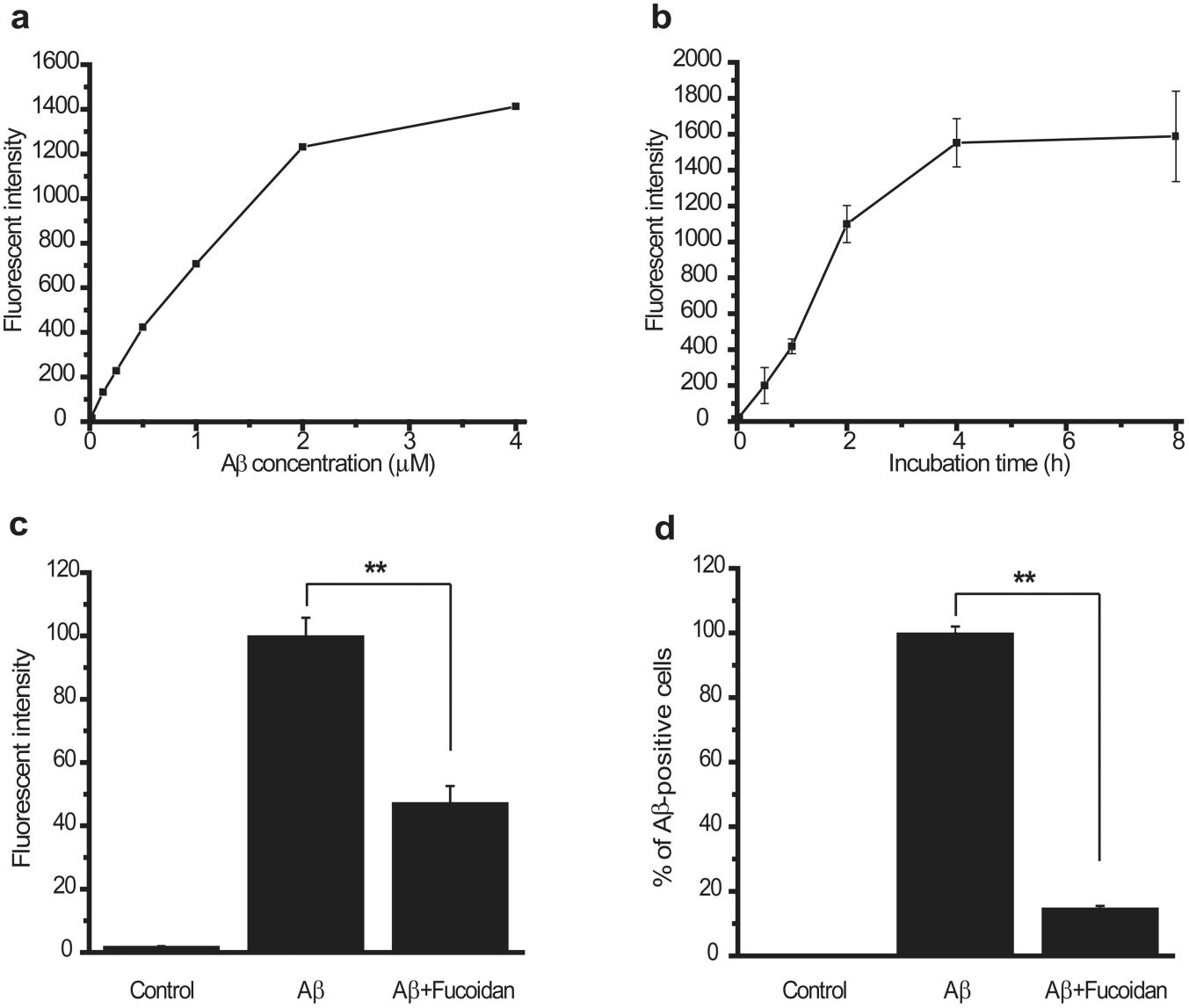

Figure 2. Uptake of sAβ by N9 microglia

(a, b) Uptake of Hilytefluor488-labeled sAβ by N9 microglia is saturable in a dose and time-dependent manner. **(c, d)** N9 cells were pretreated with 200μg/ml Fucoidan, a broad inhibitor of scavenger receptors, and then incubated with 1μM freshly dissolved Hilytefluor488-labeled sAβ 1–42 for 2 hours. The uptake of sAβ was measured by flow cytometry. Fucoidan significantly inhibited the amount of sAβ taken up by N9 cells and the number of cells that took sAβ indicating that microglial scavenger receptors are essential for phagocytosis of soluble Aβ. Values are mean ± SEM. n=3 (ANOVA** $p<0.05$)

NIH-PA Author Manuscript

NIH-PA Author Manuscript

NIH-PA Author Manuscript

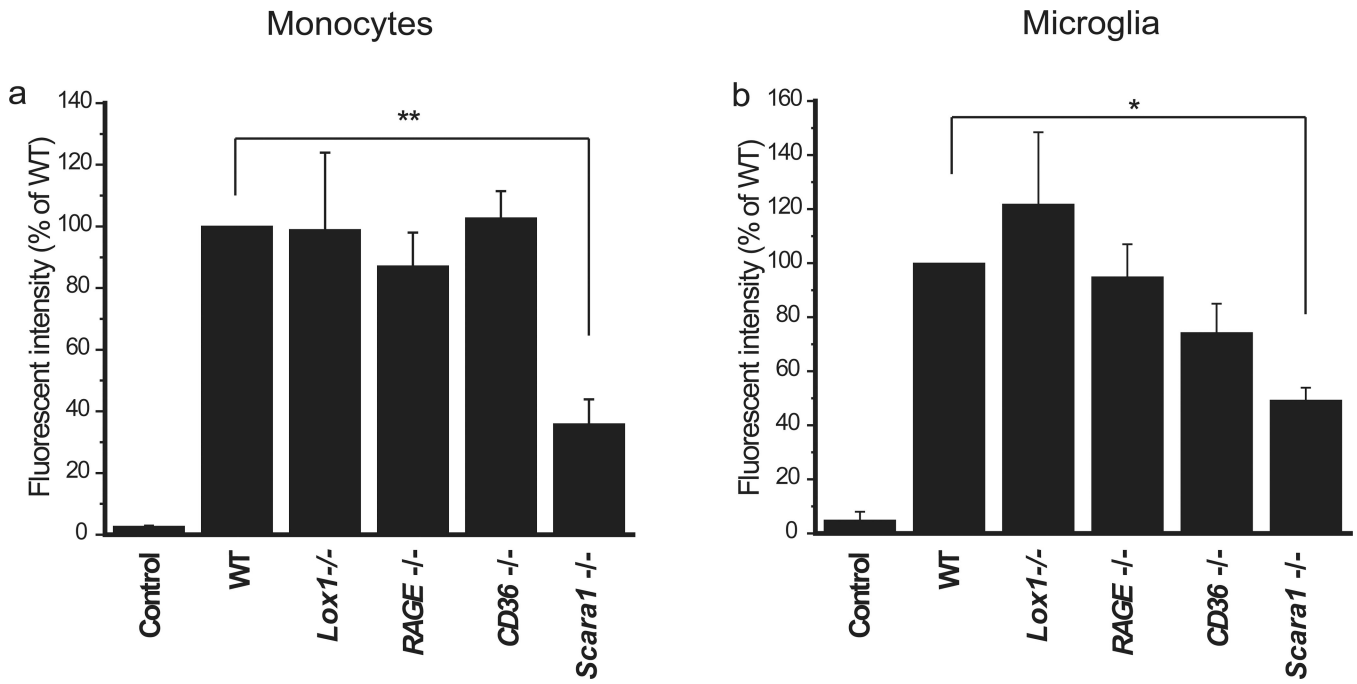

Figure 3. Scara1 is a major monocyte and microglial receptor for sAβ

Targeted deletion of *Scara1*, but not *CD36, LOX-1*, or *RAGE*, significantly reduces sAβ uptake by CD11b+ monocytes **(a)** and microglia **(b)**. Monocytes and microglia isolated from C57BL6 mice or mice with targeted deletion of the indicated gene were incubated with 1μM Hilyte fluor 488-labeled sAβ 1–42 for 2 hours, and uptake of sAβ was measured by flow cytometry. Data points represent the mean of triplicate determinations ± SEM, n=4. (ANOVA, * $p<0.05$, ** $p<0.03$)

NIH-PA Author Manuscript

NIH-PA Author Manuscript

NIH-PA Author Manuscript

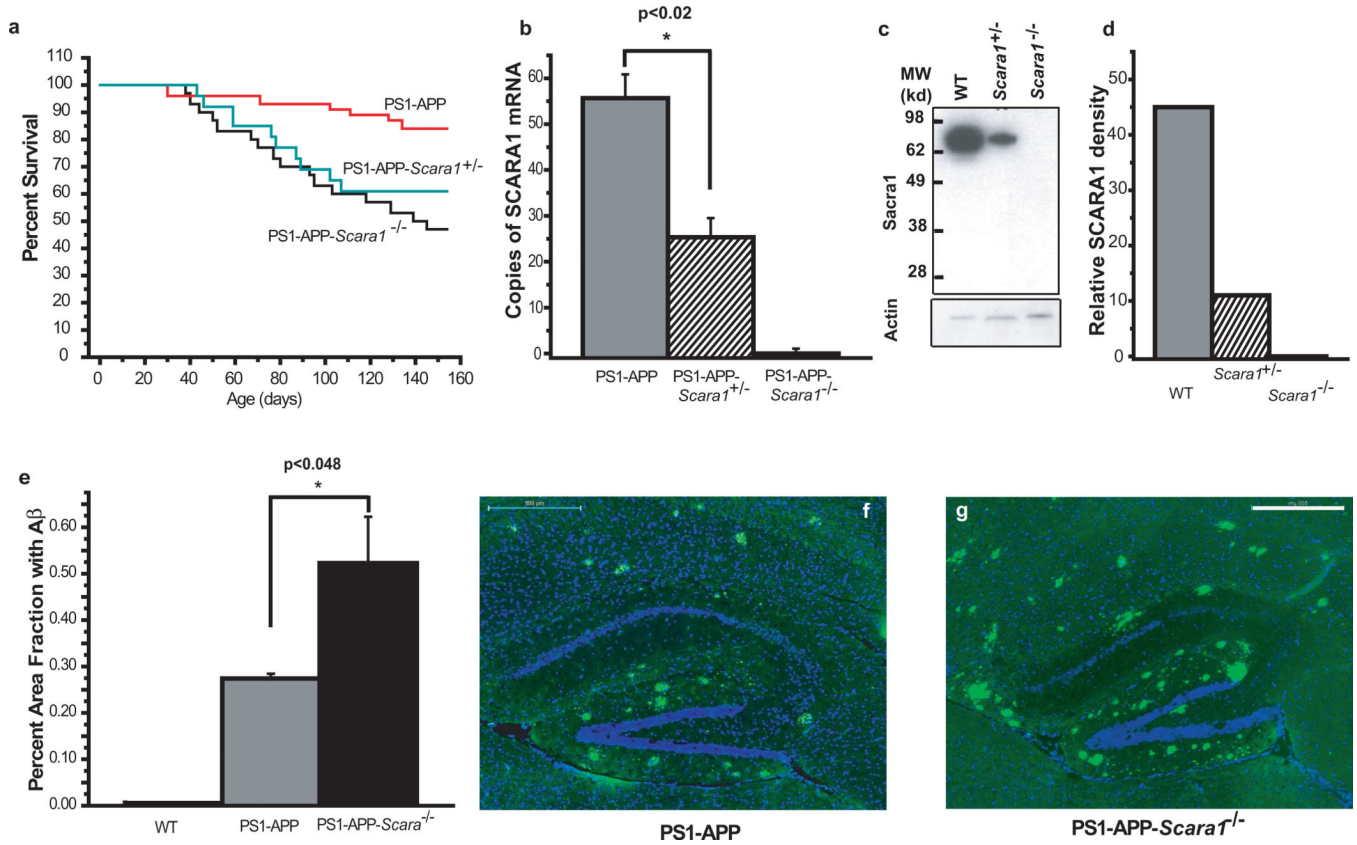

Figure 4. *Scara1* deficiency is associated with increased mortality and higher Aβ deposition in PS1-APP mice

(a) Survival curves for PS1-APP (n=30), PS1-APP-*Scara1*$^{-/+}$ (n=25) and PS1-APP-*Scara1*$^{-/-}$ (n=24) mice. **(b)** Level of *Scara1* mRNA in PS1-APP-*Scara1*$^{+/-}$ mice is 45% that of PS1-APP mice. **(c)** Reduced gene dosage in *Scara1*$^{+/-}$ *mice* is associated with a 76% reduction in *Scara1* protein levels as shown in this representative Western blot **(c)** and quantified by densitometry **(d)**, representative blot and quantification were repeated 3 different times with similar results. **(e–g)** *Scara1* deficiency significantly increases Aβ deposition in 8 month-old PS1-APP mice. Increased number of visible Aβ deposits in PS1-APP-*Scara1*$^{-/-}$ brains **(g)** compared to PS1-APP brains **(f)**. Scale bars = 500μm. Data points represent the average of 5 independent determinations per mouse, ± SEM, n=4–6 mice per group. (ANOVA, *p<0.02, **p<0.048)

NIH-PA Author Manuscript

NIH-PA Author Manuscript

NIH-PA Author Manuscript

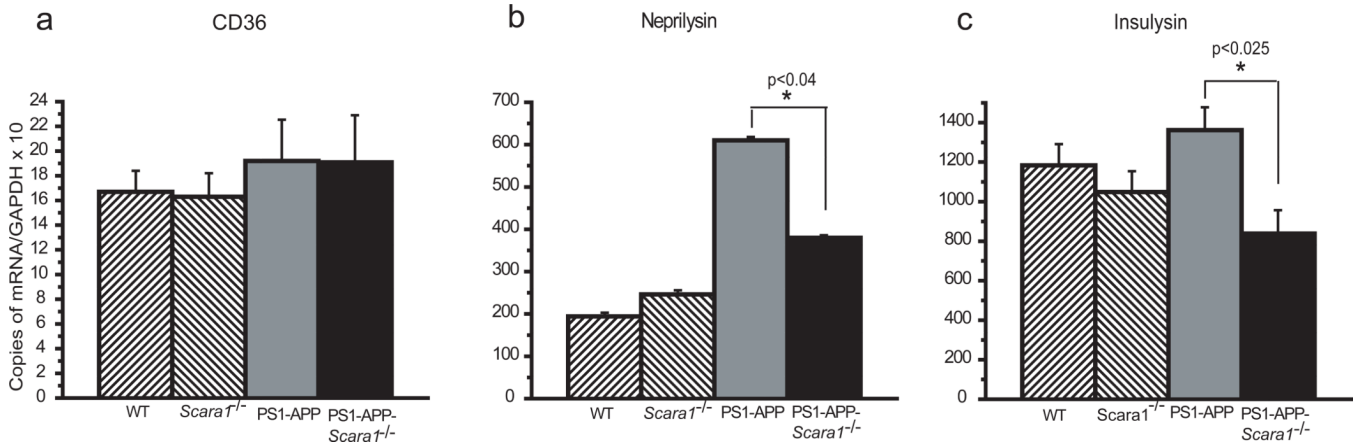

Figure 5. Effect of *Scara1* deficiency on CD36 and Aβ degrading enzymes

WT and *Scara1*$^{-/-}$ mice express comparable mRNA levels of CD36 **(a)**, and the Aβ degrading enzymes neprilysin **(b)** and insulysin **(c)** in their brains. In contrast, PS1-APP-*Scara1*$^{-/-}$ mice express similar mRNA levels of CD36 as compared to PS1-APP mice **(a)**, but significantly lower levels of neprilysin **(b)** and insulysin **(c)**. Each bar is the average of 3 triplicate determinations per mouse from 3–5 different mice per genotype ± SEM. (ANOVA*$p<0.04$, **$p<0.025$)

NIH-PA Author Manuscript

NIH-PA Author Manuscript

NIH-PA Author Manuscript

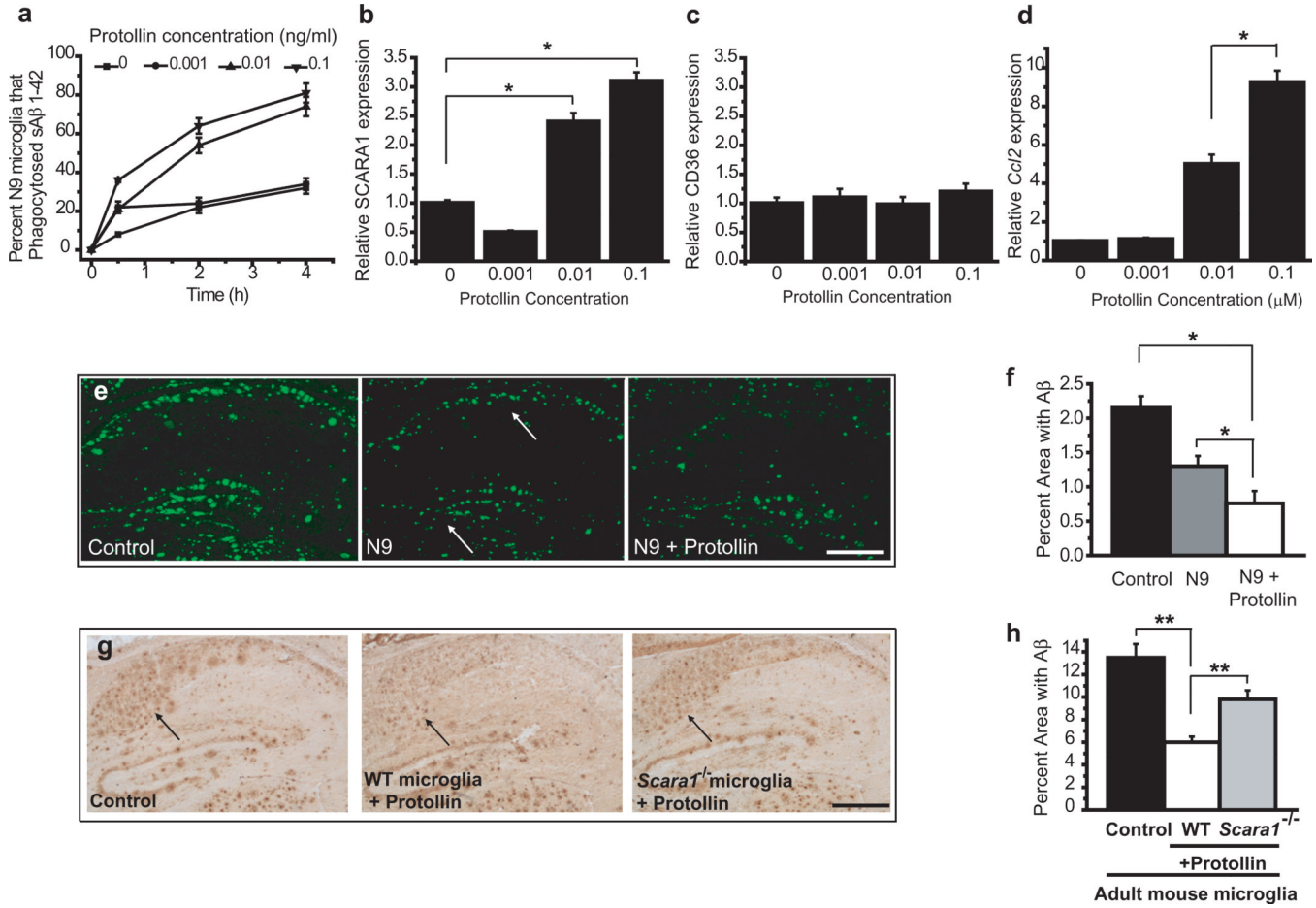

Figure 6. Upregulation of *Scara1* increases sAβ uptake *in vitro* and *in situ* in a *Scara1*-dependent mechanism

(a) Protollin, a proteosome-based adjuvant comprised of purified outer membrane proteins of *Neisseria meningitides* and lipopolysaccharide that is well tolerated in humans, upregulates sAβ uptake in N9 microglia. Cells were incubated for 18 hours in presence of different concentrations of Protollin, and incubated with 0.5 μg/ml sAβ1–42, Hilyte-fluor 488 labeled, for 30 min, 2h and 4h incubation. Cell associated sAβ was measured by flow cytometry. **(b, c)** Protollin upregulates *Scara1* but not CD36 expression at the transcriptional level as measured by qPCR. **(d)** Protollin upregulates expression of *Ccl2* in a dose-dependent manner. N9 microglia were incubated with the indicated concentration of Protollin for 24 hours, and expression of *Scara1, CD36* or *Ccl2* was quantified by qPCR. **(e, f)** N9 microglia cells are plated on brain sections from a mouse model of AD for 24h ±Protollin. The percent of the surface area of the brain covered by Aβ was measured by staining with anti-Aβ antibodies. **(g, h)** Reduction of amyloid load in the hippocampus following 24h incubation with microglia is *Scara1* dependent. Adult microglia isolated from WT and *Scara1*$^{-/-}$ mice were added to brain sections from a mouse model of AD and incubated for 24h ±Protollin. The percent of the surface area of the brain covered by Aβ was measured by staining with anti-Aβ antibodies. Scale bars=500μm. All data points represent the average of 4 independent determinations ± SEM. (ANOVA* $p<0.05$, ** $p<0.03$)